# The effect of subgrain mobility on recrystallization kinetics: phase-field simulation study



# The effect of subgrain mobility on recrystallization kinetics: phase-field simulation study

**O Abramova[1], A Prahs[2], D Schneider[1,2,3] and B Nestler[1,2,3]**

[1] Institute of Nanotechnology - Microstructure Simulations (INT-MS), Karlsruhe Institute of Technology (KIT), Karlsruhe, Germany
[2] Institute for Applied Materials - Microstructure Modelling and Simulation (IAM-MMS), Karlsruhe Institute of Technology (KIT), Karlsruhe, Germany
[3] Institute of Digital Materials Science (IDM), Karlsruhe University of Applied Sciences, Karlsruhe, Germany

E-mail: olena.abramova@kit.edu

**Abstract.** The influence of grain boundary mobility on the recrystallization process (ReX) was investigated in this study using the phase-field approach. In accordance with the Read-Shockley equation, for the interfacial mobility as a function of the misorientation angle, the resulting microstructural evolution was studied. It was observed that the disappearance of low-angle grain boundaries (LAGBs) during the ReX process caused high-angle grain boundaries to move faster during the subsequent ReX stages. For materials with high stacking energy, such as aluminum, LAGBs were additionally found to play a significant role in the ReX process. The kinetics of the ReX process, coupled with grain growth, showed the typical behavior observed in fine-grained structures of pure aluminum.

## 1. Introduction

The prediction of the recrystallization (ReX) process in the technological processes of deformation and heat treatment of metals is of decisive importance for the precise control of the mechanical properties of the resulting components and their optimization. Recrystallization that occurs during deformation is referred to as dynamic recrystallization [1], while recrystallization that occurs after deformation is called static recrystallization [2]. The use of a digital twin/surrogate to simulate recrystallization by means of the phase-field method allows to predict changes of the microstructure that determine effective material properties, such as strength, for both static [3, 4] and dynamic recrystallization [5]. Moreover, the application of the phase-field method allows the movement of grain boundaries, taking into account several driving forces. For example, grain boundary motion can be predicted based on ReX coupled with grain growth. The motion at the grain boundary is affected by two types of energy. First, there is excess of energy, due to the highly disordered nature of the grain boundary itself. Second, there is a difference in the free energy stored in neighbouring grains during deformation. Each of these energy contributions has a different effect on the process. During the formation of recrystallization nuclei, their kinetics are mainly determined by the curvature of the grain boundary, followed by the influence of the stored energy.

In this paper, we focus on the morphological evolution, due to the static recrystallization process, which occurs in two steps: First, recrystallization nuclei appear in a highly deformed

material, driven by the reduction of accumulated stress and leading to the formation of fine grains. This is followed by grain growth, which is driven by the need of the microstructure to minimize its total free energy. To calibrate the phase-field parameters associated with the free energy of the grain boundaries, it is necessary to characterize the grain boundaries as high-angle grain boundaries (HAGB) and low-angle grain boundaries (LAGB). While HAGBs have an angle of misorientation that is greater than a certain transition value, denoted by the transition angle $\Theta_m$, LAGBs have an angle of misorientation that is less than $\Theta_m$. For materials with a cubic crystal lattice, $\Theta_m = 15°$ is generally considered [6, 7]. In papers [6, 7], the choice of $\Theta_m \approx 15°$ leads to a good agreement with the available experimental data of [8]. For misorientation angles smaller than $\Theta_m$, the grain boundary energy shows a logarithmic dependence on the misorientation angle $\Theta$, which is described by the Read-Shockley equation:

$$M_{\alpha\beta}(\Theta) = M_m \left[1 - \exp^{\left(-B\left(\frac{\Theta}{\Theta_m}\right)^n\right)}\right] \tag{1}$$

cf., e.g., [9], where $M_m$ denotes the mobility of a HAGB and $M_{\alpha\beta}$ represents the mobility between the phases $\alpha$ and $\beta$. With small misorientation angles, in particular, the mobility as well as the interfacial energy density almost disappear, as shown in figure 1. The difference in the mobility of LAGBs and HAGBs can be explained by different mechanisms that characterize boundary migration. While dislocation interactions and motions occur at low-angle interfaces, atomic jumps are present at high-angle interfaces. At large misorientation angles, which are typical for HAGBs, the mobility of the GBs reaches a steady-state value. The steady-state region shifts depending on the value of the exponent $n$, which is illustrated by the horizontal tangent in figure 1 (b). For $\Theta \in [0°, \Theta_m]$, the shape of the distribution of $M_{\alpha\beta}(\Theta)$ is significantly influenced by the parameters $B$ and $n$, which are referred to as [10]. It should be noted that $B$, $n$, and $\Theta_m$ are strongly dependent on the material and the annealing temperature. In addition, the GB mobility $M_m$ for $\Theta \in [0°, 40°]$ increases significantly, compared to a pure aluminum bicrystal, cf. e.g. [11].

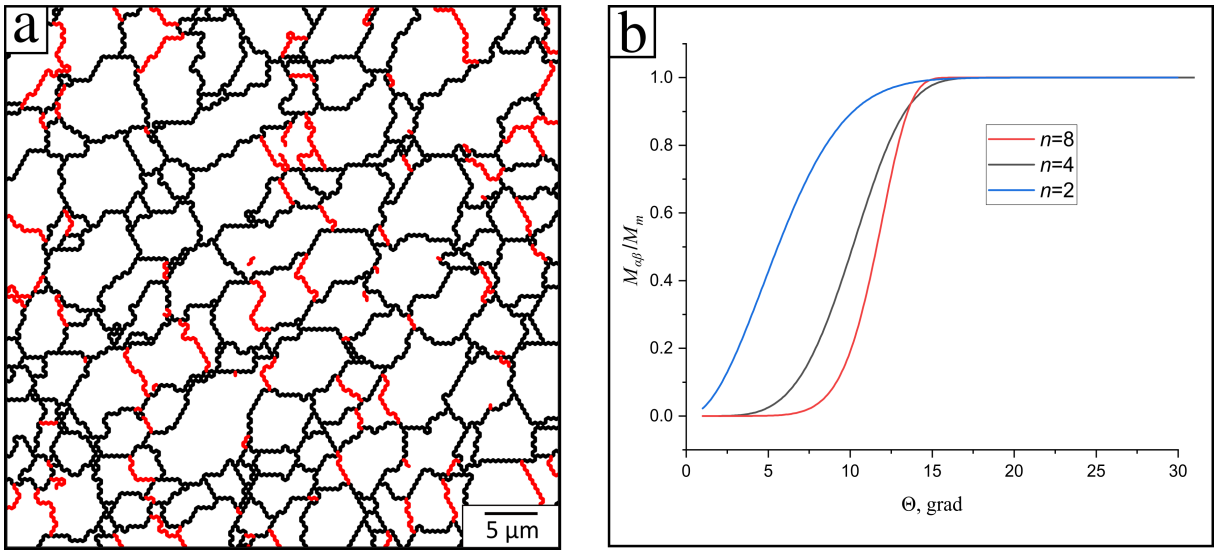


**Figure 1.** Grain boundary network (a) and grain boundary mobility (b) as a function of misorientation of crystal lattices (equation 1) between two grains for $M_{\mathrm{HAGB}} = 10^6$ m$^4$(Js)$^{-1}$. Above the misorientation of $\Theta_m = 15°$, the value is constant. HAGBs are marked in black, while LAGBs are marked in red.

Experimental measurements [12, 13] prove that grain boundary motion strongly depends on the misorientation of neighboring grains, as discussed by Gottstein [12]. For LAGBs, the shape of the distribution of $M_{\alpha\beta}$ is still the subject of current research. Given the complex process of grain boundary (GB) migration during recrystallization (ReX), certain GBs exhibit varying migration rates. HAGBs with similar mobility can move at different speeds due to differences in their shapes and, consequently, their surface energies. The role of the HAGB/LAGB fraction in the initial state is still not clear. This motivates the simulation study of recrystallization with the MPFM, considering a digital microstructure that mimics the experimentally determined microstructure of a UFG material. The aim of the present work is to investigate the effect of the GB mobility dependence in the LAGB region on the ReX kinetics, using the PFM in the software package PACE3D [14], according to the Read-Shockley equation.

## 2. Initial microstructure and Read-Shockley equation parameters

The influence of the exponent $n$ on grain growth is investigated for one initial microstructure.

The initial microstructure generated by the Voronoi tessellation algorithm of Vondrous et al. [4], with a physical domain size of $55\times50$ µm, discretized by $316\times287$ voxels, is shown in figure 1 (a). The size of subgrains with LAGBs (D) is evaluated using the equal diameter method [15], with area fraction-weighted specific fractions and a critical angle of misorientation of 2 degrees. The initial grain orientations are chosen randomly, with the misorientation angle between neighboring grains varying from one to 62°, as is typically the case in isotropic *fcc* polycrystals [13]. The structures with a dominant fraction of HAGBs are characteristic of materials after strong plastic deformation [16, 17].

The choice of the exponent $n$ significantly affects the shape of the distribution of $M(\Theta)$ (figure 1 (b)). For $n = 8$, the mobility of boundaries with a misorientation of less than 7° is close to zero, while the mobility of boundaries with a misorientation of less than 5° is zero. Decreasing the value of $n$ to 4 and 2, respectively, leads to a significant mobility of the boundaries in the range of $5° - 15°$ and $0° - 10°$, respectively.

## 3. Model description

A multicomponent multiphase-field model presented by Nestler et al. [18] is used to simulate the recrystallization process, which includes the Read-Shockley [3, 19] interfacial energy variation in combination with the Humphreys [20] interfacial mobility variation. To account for the stored energy in the system, which acts as a driving force for grain recrystallization and reduces the deformation-induced dislocations in a system, an additional bulk energy term is included, following the approach of Vondrous et al. [4]. The free energy functional then becomes:

$$\begin{aligned} \mathcal{F} &= \int_V f \,\mathrm{d}V = \int_V (W_{\mathrm{intf}} + \overline{W}_{\mathrm{bulk}}) \,\mathrm{d}V, \\ W_{\mathrm{intf}} &= \varepsilon a(\boldsymbol{\phi}, \boldsymbol{\nabla}\boldsymbol{\phi}) + \frac{1}{\varepsilon}\omega(\boldsymbol{\phi}), \quad \overline{W}_{\mathrm{bulk}} = f_{\mathrm{RX}}(\boldsymbol{\phi}, \rho_d), \end{aligned} \tag{2}$$

where $W_{\mathrm{intf}}$ is the interfacial free energy density and $\overline{W}_{\mathrm{bulk}}$ is the bulk contribution to the free energy density. The N-tuple of continuous order parameters is denoted by $\boldsymbol{\phi} = \{\phi_1, \ldots, \phi_\alpha, \ldots, \phi_N\}$, where each order parameter $\phi_\alpha(\boldsymbol{x}, t)$ represents the volume fraction of a particular phase $\alpha$. The interfacial energy density is composed of the gradient contribution $\varepsilon a(\boldsymbol{\phi}, \boldsymbol{\nabla}\boldsymbol{\phi})$ and the multi-obstacle type potential $\omega(\boldsymbol{\phi})/\varepsilon$. According to Nestler et al. [18], the gradient energy density is defined as:

$$\varepsilon a(\boldsymbol{\phi}, \boldsymbol{\nabla}\boldsymbol{\phi}) = \varepsilon \sum_{\alpha<\beta} \gamma_{\alpha\beta} |\phi_\alpha \boldsymbol{\nabla}\phi_\beta - \phi_\beta \boldsymbol{\nabla}\phi_\alpha|^2, \tag{3}$$

where $\gamma_{\alpha\beta}$ denotes the interfacial energy density between the phases $\alpha$ and $\beta$. For a detailed description of the multi-obstacle potential $\omega(\boldsymbol{\phi})$, see, e.g., [18, 14].

The bulk energy density term $\overline{W}_{\text{bulk}}$, which is a function of the dislocation density $\rho_d$, represents the stored energy of the system and is defined as follows:

$$\overline{W}_{\text{bulk}}(\boldsymbol{\phi}, \rho_d) = W_{\text{bulk}}(\rho_d) \sum_{\alpha}^{N} m_\alpha h(\phi_\alpha), \tag{4}$$

$$W_{\text{bulk}}(\rho_d) = \frac{1}{2} \rho_d G b^2, \tag{5}$$

where $G$ is the shear modulus and $b$ is the Burgers vector [19]. The interpolation function $h(\phi_\alpha)$ to distinguish the locally present grain state is selected as: $h(\phi_\alpha) = \phi_\alpha$. The phase-inherent storage parameter $m_\alpha$ is related to the conventional theory of the static ReX. $m_\alpha$ indicates whether a phase recrystallizes or not, in the sense that $m_\alpha = 0$ refers to phase with zero bulk energy, while $m_\alpha = 1$ indicates a non-zero bulk energy phase. Once a cell is fully recrystallized, the stored energy becomes zero. Consequently, $\overline{W}_{\text{bulk}}$ decreases as a recrystallizing phase grows. Considering the volume constraint $\sum_\alpha \phi_\alpha = 1$, the evolution equation according to the variational approach of Steinbach and Pezzolla [21] is:

$$\frac{\partial \phi_\alpha}{\partial t} = -\frac{1}{\epsilon \tilde{N}} \sum_{\beta \neq \alpha}^{\tilde{N}} M_{\alpha\beta}(\Theta) \left[ \frac{\delta f}{\delta \phi_\alpha} - \frac{\delta f}{\delta \phi_\beta} \right], \quad \forall \phi_\alpha, \alpha = 0, ..., \tilde{N}, \tag{6}$$

where $\tilde{N}$ denotes the number of locally active phases. In this context, the variational derivative is used, which reads as follows:

$$\frac{\delta f}{\delta \phi_\alpha} = \frac{\partial f}{\partial \phi_\alpha} - \text{div} \left[ \frac{\partial f}{\partial \boldsymbol{\nabla} \phi_\alpha} \right], \tag{7}$$

where $\boldsymbol{\nabla} \phi_\alpha$ is the gradient of the order parameter $\phi_\alpha$ and $\text{div}(\cdot)$ represents the divergence operator.

Without the contribution of the stored energy in the bulk, the grain boundary migration occurs due to the curvature minimization of the grain boundaries (GBs). Consequently, the migration velocity of the GB is governed by the decrease of the free energy, due to the decrease of the area surrounded by the GB. In this context, the experiments of [22] show that the migration of the radial velocity $\dot{R}$ of an inclusion with a radius $R$ is proportional to the curvature of the interface $1/R$:

$$\dot{R} \sim \frac{\gamma M_{\alpha\beta}}{R}, \tag{8}$$

where $M_{\alpha\beta}$ denotes the mobility and $\gamma$ is the grain boundary energy (per unit area).

## 4. Simulation results

### *4.1. Simulation setup*

For an initially fine-grained polycrystalline microstructure, the influence of the exponent $n$ on grain growth is discussed here by using multiphase-field simulations (MPFM). To discuss normal grain growth, the evolution of the initial microstructure is simulated for different values of the exponent $n$ and compared after $10^3$ and $50 \times 10^3$ time steps. The results are shown in figure 2.

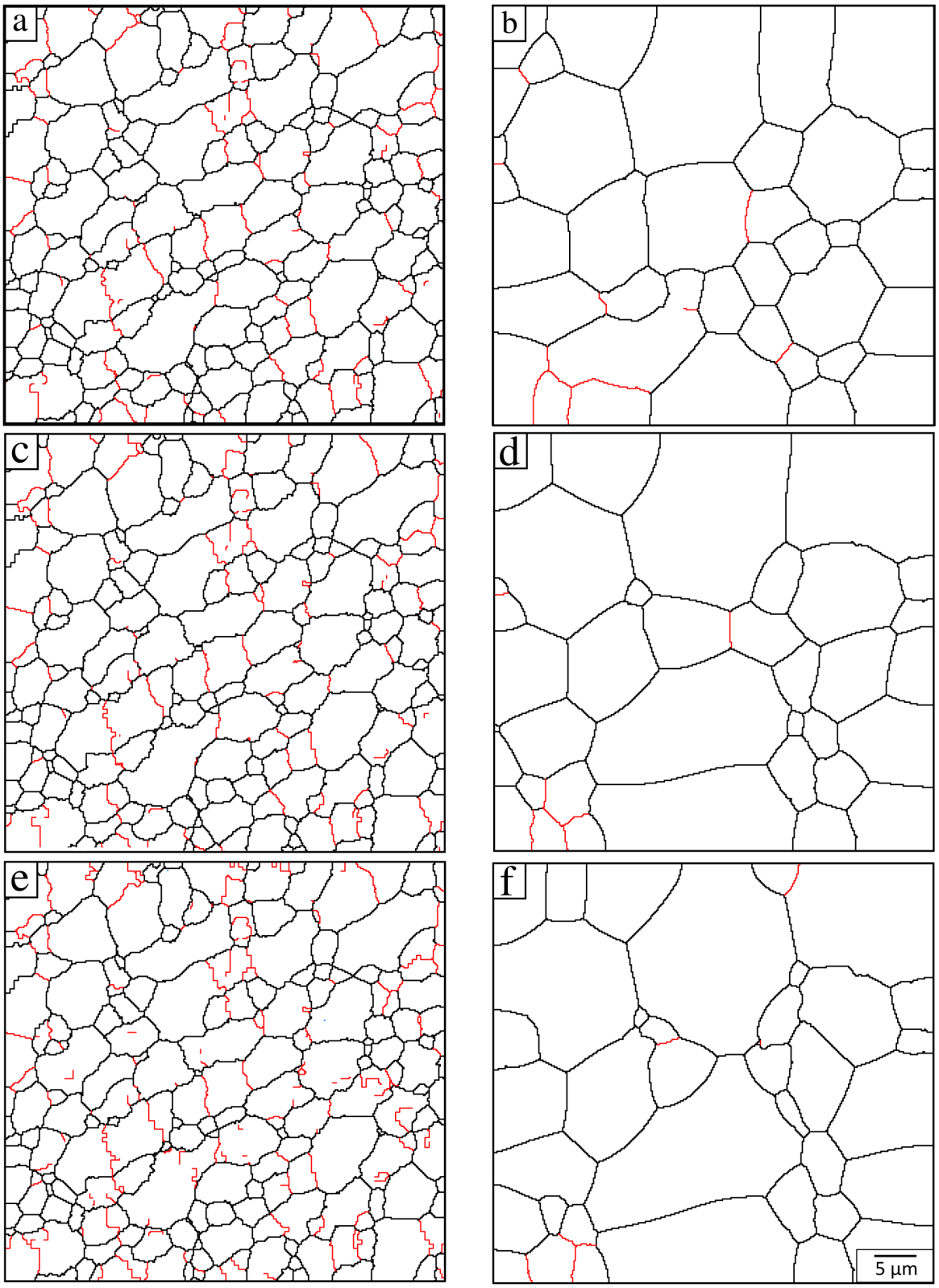


**Figure 2.** Simulated structures after $10^3$ (a, c, e) and $50 \times 10^3$ (b, d, f) steps calculated in PACE3D, using values of parameter $n = 2$ (a, b), 4 (c, d) and 8 (e, f). HAGBs are marked in black, while LAGBs are marked in red.

*4.2. Influence of the exponent n*

The simulated structures after $10^3$ steps of the MPFM calculation with different $n$ values show a high degree of similarity (figure 2 (a, c, e)). After $50 \times 10^3$ time steps, a significant grain growth with different grain shapes and D grain sizes can be observed, as shown in figure 2 (b, d, f). For the considered values of the exponent $n$, the number and length of the LAGBs decreases as the number of calculation steps increases from $10^3$ to $50 \times 10^3$. The corresponding values for the grain size and the volume fraction of the HAGBs are given in table 1.

It should be noted that the mechanism of ReX provided by the considered multiphase-field model is a movement of the GB of pairwise grains, $\alpha$ and $\beta$, towards the region of higher stored energy [4]. The gradient of stored energy (SE) prevents grains with high SE from moving forwards and, eventually, merging with other grains that also exhibit SE. Grains with low SE, which are located between grains with high SE and have a different orientation, merge with these grains, when the grain boundaries of two grains, $\alpha$ and $\beta$, move towards the region of higher stored energy. Abrivard et al. [11] have clearly confirmed that at the end of the recrystallization process, the grains with the lowest energy content predominate. In the specific example related to static recrystallization, the relationship between the growth of the grain boundaries and their shape was studied to determine the speed of their movement, as described in equation (8). The analysis focused on the curvature of the interface $\dot{R}$, which served as the main driving force in the calculations.

In the structures observed after $50 \times 10^3$ calculation steps (figure 2 (b, d, f)), the largest grains are characterized by straight grain boundaries (GBs) and triple junctions with angles close to 120°. Figure 2 indicates that the slow LAGBs vanish for all three considered ReX kinetics. This can be attributed to the underlying mechanism of gradual assimilation into grains with HAGBs, which is closely associated with the interface energy between the grains. According to the Read-Shockley model [19], the interface energy $\Delta\Theta_{\alpha\beta}$ is a function of the misorientation angle $\Delta\Theta_{\alpha\beta}$ between the grains $\alpha$ and $\beta$, given by

$$\gamma_{\alpha\beta}(\Delta\Theta_{\alpha\beta}) = \begin{cases} \gamma_{\mathrm{HAGB}} \frac{\Delta\Theta_{\alpha\beta}}{\Delta\Theta_m} \left(1 - \ln \frac{\Delta\Theta_{\alpha\beta}}{\Delta\Theta_m}\right), & \Delta\Theta_{\alpha\beta} < \Delta\Theta_m \\ \gamma_{\mathrm{HAGB}}, & \text{else.} \end{cases} \tag{9}$$

In this context, $\gamma_{\mathrm{HAGB}}$ is the interfacial energy of a HAGB. The transition from a LAGB to a HAGB takes place at $\Delta\Theta_m = 15°$. Thus, for LAGBs the interface energy is significantly smaller compared to HAGBs according to the Read-Shockley model. The small interface energy leads to a higher impact of the curvature minimization. Consequently, the grains characterized by slow LAGBs are progressively incorporated into grains with higher interface energy, constituting the final microstructure at the end of the ReX process. This observation aligns well with previous findings reported by Abrivard et al. [11], further supporting that grains with the lowest energy content predominate at the end of the recrystallization process. Moreover, the shape of the function $M_{\alpha\beta}(\Theta)$ at $n = 2$ is also typical for metals with high stacking fault energy. In an experimental study on aluminum Yang et al. [8], a similar grain size distribution as in the simulation was also observed. This suggests that the results obtained are in agreement with the experimental results. It is also worth noting that the grain boundary mobility function $M_{\alpha\beta}(\Theta)$ is significantly affected by temperature. In pure nickel, for example, LAGBs exhibit a higher mobility at high temperatures than HAGBs [23]. The variation of the $n$ value in the $M_{\alpha\beta}(\Theta)$ function (equation (1)) can be obtained in aluminum-based solid solutions with different alloying elements, which can affect the grain boundary energy and mobility, resulting in variations in grain growth behavior.

**Table 1.** Microstructure parameters simulated with PACE3D: number of calculated steps (N, ×100), the subgrain size D, the volume fraction of HAGBs $V_{HAGBs}$.

| $n$ | 2 | | | | | 4 | | | | | 8 | | | | |
|---|---|---|---|---|---|---|---|---|---|---|---|---|---|---|---|
| N, ×100 | 10 | 50 | 100 | 300 | 500 | 10 | 50 | 100 | 300 | 500 | 10 | 50 | 100 | 300 | 500 |
| D, ($\mu m$) | 2.1 | 2.6 | 3.2 | 4.3 | 5.2 | 2.1 | 2.6 | 3.1 | 4.0 | 5.0 | 2.0 | 2.5 | 3.1 | 4.0 | 4.8 |
| $V_{HAGBs}$, % | 82.9 | 86.0 | 90.0 | 90.1 | 90.5 | 82.5 | 85.7 | 89.3 | 90.0 | 94.5 | 82.2 | 84.3 | 86.9 | 90.4 | 95.4 |

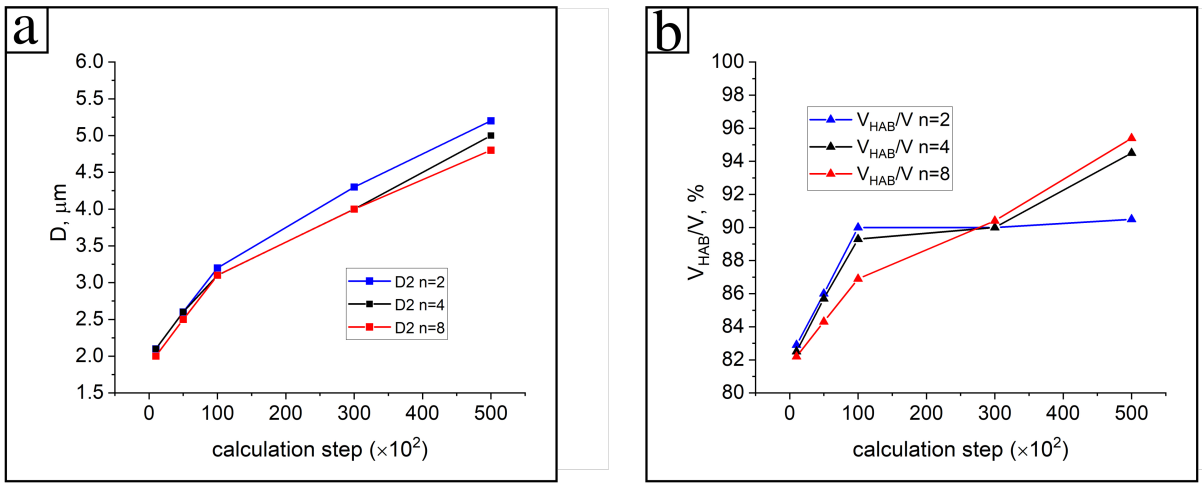


**Figure 3.** Evolution of the microstructure parameters during recrystallization: tendencies of the grain size D (a) and the fraction of high-angle boundaries $V_{HAGB}$ (b).

*4.3. Statistical analysis of n influence on grain growth*

The tendencies of the D and $V_{HAGB}$ - specific fractions for the simulations with different $n$ values are shown in figure 3. The comparatively small volume fraction of LAGBs in the initial structure (figure 1 (a)) decreases with increasing time steps. This leads to an increase of $V_{HAGBs}$ =$V_{HAGBs}$/V from 78% to $90-95\%$, after $50 \times 10^3$ time steps, as shown in figure 3.

For the chosen exponents ($n = 2$ and $n = 8$), the largest deviations in the distribution of the volume fraction of HAGBs ($V_{HAGBs}$/V) are observed at the time steps $10^3$ and $50 \times 10^3$. Consequently, the most significant difference in recrystallization kinetics is observed when $V_{HAGBs}$ =$V_{HAGBs}$/V reaches saturation at about 90%, after calculations with $n = 2$. The graph in figure 3 shows the saturation of $V_{HAGB}$ at about 90%, after calculations with $n = 2$, and a nearly linear dependence after calculations with $n = 4$ and $n = 8$ (figure 3).

Varying the exponent $n$ has no significant effect on grain growth, as measured by the parameter D. Lower values of $n$, however, correspond to higher values of D. The highest value of D is obtained after $50 \times 10^3$ time steps, using $n = 2$, as shown in figure 3 and documented in table 1.

*4.4. Further remarks*

In contrast to other methods used for the simulation of ReX, e.g., the Monte Carlo method [24, 25] and various other analytical models [26, 27, 28], the applied approach accounts for the dependency of the GB mobility on the misorientation angle by means of the Read-Shockley approach as discussed by [4].

In contrast to the simulations carried out by [4], different exponents for the Read-Shockley equation and, thus, different ReX kinetics are considered, in this work. These new insights allow us to compare our findings with Abrivard's publication [11], which discusses the MPFM on structures with saturated GB mobility up to 10 degrees.

The further development of MFPM for ReX simulation may consider involving a more complex $M_{\alpha\beta}(\Theta)$ dependence in the HAGB range [29]. However, it is essential to highlight the slight effect of the critical falling angle of mobility in the LAGB range observed in this work.

## 5. Conclusion

The kinetics of recrystallization and grain growth predicted in figure 3 shows a typical behavior observed in pure aluminum, especially when it has undergone severe plastic deformation. Interestingly, the significant difference in the mobility of the LAGBs, set with the parameter $n$ within the Read-Shockley equation, has no noticeable effect on the kinetics of recrystallization. Both the specific fraction $V_{HAGBs}$ and the grain size D show similar growth tendencies. Although the present simulation studies are performed in 2D, extending the analysis to three-dimensional phenomena would provide a more comprehensive understanding of the evolution of the microstructure and will be the content forthcoming studies applying the MPFM framework.

## Acknowledgments

The authors gratefully acknowledge financial support for this research through the initiative "Virtual Materials Design" within the programme "Material Systems Engineering (MSE)" (No. 43.31.01) of the Helmholtz Association. Data and data processing are provided within the framework of the KNMFi and MDMC initiatives (No. 43.31.01), through the research data infrastructure Kadi4Mat `https://kadi.iam.kit.edu.`

## References

[1] Sakai T, Belyakov A, Kaibyshev R, Miura H and Jonas J J 2014 *Progr. in Mater. Scien.* **60** 130 ISSN 0079-6425 URL `http://www.sciencedirect.com/science/article/pii/S0079642513000698`
[2] Humphreys F J and Hatherly M 2012 *Recryst. and related annealing phenom.* (Elsevier) ISBN 008098388X
[3] Vondrous A, Bienger P, Schreijäg S, Selzer M, Schneider D, Nestler B, Helm D and Mönig R 2015 *Comput. Mech.* **55** 439 ISSN 1432-0924 URL `https://doi.org/10.1007/s00466-014-1115-0`
[4] Vondrous A, Reichardt M and Nestler B 2014 *Model. and Sim. in Mater. Scien. and Eng.* **22** 025014 ISSN 0965-0393
[5] Li Y, Hu S, Barker E, Overman N, Whalen S and Mathaudhu S 2020 *Comput. Mat. Scien.* **180** 109707 ISSN 0927-0256
[6] Sutton A P and Balluffi R W 1995 *Interfaces in Crystalline Mater.* (Oxford: Clarendon Pr.)
[7] Gottstein G and Shvindlerman L 2009 *Grain Boundary Migration in Metals: Thermodynamics, Kinetics, Applications, 2nd Ed.* Mater. Scien. & Techn. (CRC Press) ISBN 9781439858998 URL `https://books.google.de/books?id=kphAaSm14ucC`
[8] Yang C C, Rollett A D and Mullins W W 2001 *Scr. Mater.* **44** 2735 ISSN 1359-6462
[9] Humphreys F 1997 *Acta Mater.* **45** 4231 ISSN 1359-6454 URL `https://www.sciencedirect.com/science/article/pii/S1359645497000700`
[10] Shockley W and Read W T 1949 *Phys. Rev.* **75** 692
[11] Abrivard G, Busso E P, Forest S and Appolaire B 2012 *Philos. Mag.* **92** 3643 ISSN 1478-6435 URL `https://doi.org/10.1080/14786435.2012.717726`
[12] Gottstein G and a Molodov D 2001 *Recryst. and grain growth* (Springer-Verlag) ISBN 3540418377
[13] Mackenzie J K 1964 *Acta Metal.* **12** 223 ISSN 0001-6160
[14] Hötzer J, Reiter A, Hierl H, Steinmetz P, Selzer M and Nestler B 2018 *Jour. of Computat. Scien.* **26** 1 ISSN 18777503 URL `http://linkinghub.elsevier.com/retrieve/pii/S1877750317310116`
[15] Voort G F V 1999 *Metallography: principles and practice* (Oxford: Mater. Park, OH: ASM Internat.)
[16] Valiev R Z, Estrin Y, Horita Z, Langdon T G, Zehetbauer M J and Zhu Y T 2016 *Mater. Res. Let.* **4** 1 ISSN null URL `https://doi.org/10.1080/21663831.2015.1060543`

[17] Zhilyaev A P and Langdon T G 2008 *Progr. in Mater. Scien.* **53** 893 ISSN 0079-6425 URL http://www.sciencedirect.com/science/article/pii/S007964250800025X
[18] Nestler B, Garcke H and Stinner B 2005 *Phys. Rev.* E **71** 041609 URL https://link.aps.org/doi/10.1103/PhysRevE.71.041609
[19] Read W T and Shockley W 1950 *Phys. Rev.* **78** 275 URL https://link.aps.org/doi/10.1103/PhysRev.78.275
[20] Humphreys F J and Hatherly M 2004 *Ch.12 - Recryst. Textures* (Oxford: Elsevier) p 379 ISBN 978-0-08-044164-1 URL https://www.sciencedirect.com/science/article/pii/B9780080441641500165
[21] Steinbach I and Pezzolla F 1999 *Phys. D: Nonlin. Phenom.* **134** 385 ISSN 0167-2789 URL https://www.sciencedirect.com/science/article/pii/S0167278999001293
[22] Upmanyu M, Srolovitz D J, Shvindlerman L S and Gottstein G 1999 *Acta Mater.* **47** 3901 ISSN 1359-6454
[23] Olmsted D L, Holm E A and Foiles S M 2009 *Acta Mater.* **57** 3704 ISSN 1359-6454
[24] Humphreys F 1992 *Mater. Science and Techn.* **8** 135–144
[25] Rollett A and Manohar P 2004 *Contin. Scale Simul. of Engin. Mater.* 855
[26] Hallberg H 2011 *Metals* **1** 16 ISSN 2075-4701 URL https://www.mdpi.com/2075-4701/1/1/16
[27] Michels A, Krill C, Ehrhardt H, Birringer R and Wu D 1999 *Acta Mater.* **47** 2143 ISSN 1359-6454 URL https://www.sciencedirect.com/science/article/pii/S1359645499000798
[28] Vandermeer R and Hansen N 2008 *Acta Mater.* **56** 5719 ISSN 1359-6454 URL https://www.sciencedirect.com/science/article/pii/S1359645408005430
[29] Gottstein G and Sebald R 2001 *J. of mater. processing techn.* **117** 282–287